0022-3565/06/3162-592–600$20.00
THE JOURNAL OF PHARMACOLOGY AND EXPERIMENTAL THERAPEUTICS
JPET 316:592–600, 2006

Vol. 316, No. 2
95042/3071616
Printed in U.S.A.

Critical Role of Plasminogen Activator Inhibitor-1 in Cholestatic Liver Injury and Fibrosis

Ina Bergheim, Luping Guo, Molly Anne Davis, Ilinca Duveau, and Gavin E. Arteel

Department of Pharmacology and Toxicology and the James Graham Brown-Cancer Center, University of Louisville Health Sciences Center, Louisville, Kentucky (I.B., L.G., M.A.D., I.D., G.E.A.)

Received September 1, 2005; accepted October 11, 2005

ABSTRACT

Plasminogen activator inhibitor-1 (PAI-1) is an acute phase protein known to correlate with hepatic fibrosis. However, whether or not PAI-1 plays a causal role in this disease process had not been directly tested. Therefore, wild-type or PAI-1 knockout (PAI-$1^{-/-}$) mice underwent bile duct ligation. Mice were sacrificed either 3 or 14 days after surgery for assessment of early (i.e., inflammation) and late (i.e., fibrosis) changes caused by bile duct ligation. Liver injury was determined by histopathology and plasma enzymes. Accumulation of extracellular matrix was evaluated by Sirius red staining and by measuring hydroxyproline content. Hepatic expression of PAI-1 was increased ~9-fold by bile duct ligation in wild-type mice. Furthermore, early liver injury and inflammation due to bile duct ligation was significantly blunted in PAI-$1^{-/-}$ mice in comparison with wild-type mice. Although PAI-$1^{-/-}$ mice were significantly protected against the accumulation of extracellular matrix caused by bile duct ligation, increases in expression of indices of stellate cell activation and collagen synthesis caused by bile duct ligation were not attenuated. Protection did, however, correlate with an elevation in hepatic activities of plasminogen activator and matrix metalloprotease activities. In contrast, the increase in tissue inhibitor of metalloproteases-1 protein, a major inhibitor of matrix metalloproteases, caused by bile duct ligation was not altered in PAI-$1^{-/-}$ mice compared with the wild-type strain. The increase in hepatic activity of urokinase-type plasminogen activator was also accompanied by more activation of the hepatocyte growth factor receptor c-Met. Taken together, these data suggest that PAI-1 plays a causal role in mediating fibrosis during cholestasis.

A common pathologic response to chronic liver disease is accumulation of extracellular matrices (ECM), leading to fibrosis and possible progression to cirrhosis. In the absence of liver transplantation, the sequelae associated with this disease often lead to death of the patient (Kim et al., 2002). It was recently shown in humans that liver fibrosis/cirrhosis can at least partially resolve if the underlying cause is effectively treated (e.g., hepatitis virus C infection) (Poynard et al., 2002). However, due in part to an incomplete understanding of the mechanisms underlying hepatic fibrosis, no Food and Drug Administration-approved therapy to halt the progression or enhance the rate of resolution of this disease has been identified.

Plasminogen activator inhibitor-1 (PAI-1) is an acute phase protein that can be induced during inflammation (Quax et al., 1990; Luyendyk et al., 2004; Lagoa et al., 2005). PAI-1 is a major inhibitor of both tissue-type plasminogen activator (tPA) and urokinase-type plasminogen activator (uPA) and, therefore, a key regulator of fibrinolysis by plasmin (Kruithof, 1988). In addition to regulating the accumulation of fibrinogen/fibrin in the extracellular space, plasmin can also directly degrade other ECM components such as laminin, proteoglycan, and type IV collagen (Liotta et al., 1981; Mochan and Keler, 1984; Mackay et al., 1990). Furthermore, plasmin can also indirectly degrade ECM via activation of MMPs (Ramos-DeSimone et al., 1999). Thus, by impairing the plasminogen activating systems, PAI-1 could significantly alter organ fibrogenesis. Indeed, a protective effect of pharmacologic/genetic prevention of PAI-1 induction has been observed in models of renal, pulmonary, and vascular fibrosis (Hattori et al., 2000; Kaikita et al., 2001; Huang et al., 2003).

Similar to other organs, PAI-1 is known to be induced in

This work was supported, in part, by a grant from the National Institute of Alcohol Abuse and Alcoholism.
Article, publication date, and citation information can be found at http://jpet.aspetjournals.org.
doi:10.1124/jpet.105.095042.

ABBREVIATIONS: ECM, extracellular matrix/matrices; PAI-1, plasminogen activator inhibitor 1; tPA, tissue-type plasminogen activator; uPA, urokinase-type plasminogen activator; MMP, matrix metalloprotease; ALT, alanine aminotransferase; AST, aspartate aminotransferase; ALP, alkaline phosphatase; RT, reverse transcription; PCR, polymerase chain reaction; C_T, threshold cycle; TIMP, tissue inhibitor of metalloproteases; MOPS, 4-morpholinepropanesulfonic acid; αSMA, α smooth muscle actin; HGF, hepatocyte growth factor; BDL, bile duct ligation; H&E, hematoxylin & eosin; E-64, *trans*-epoxysuccinyl-L-leucylamido(4-guanido)butane.

models of hepatic fibrosis (Zhang et al., 1999; Bueno et al., 2000). PAI-1 is also directly produced by hepatic stellate cells, the major cell type responsible for ECM accumulation during fibrosis, when activated in vitro (Leyland et al., 1996). Although it has been proposed that PAI-1 may contribute to fibrogenesis in liver, this hypothesis has not been directly tested in this organ. Therefore, the purpose of the current study was to determine the effect of knocking out PAI-1 on experimental liver damage and fibrosis caused by bile duct ligation in mice.

Materials and Methods

Animals and Treatments. Mice were housed in a pathogen-free barrier facility accredited by the Association for Assessment and Accreditation of Laboratory Animal Care, and procedures were approved by the local Institutional Animal Care and Use Committee. Eight-week-old male C57BL/6J and PAI-1 knockout (B6.129S2-Serpine1^{tm1Mlg}/J; PAI-1$^{-/-}$) mice were obtained from The Jackson Laboratory (Bar Harbor, ME). This knockout strain has been backcrossed at least 10 times onto C57BL/6, avoiding concerns regarding genetic differences between wild-type and strain and the knockouts at nonspecific loci. Food and tap water were allowed ad libitum. Bile duct ligation was performed by surgical ligation of the common hepatic bile duct under isoflurane anesthesia. Sham-operated mice underwent a laparotomy with exposure but not ligation of the common bile duct. Animals were anesthetized with sodium pentobarbital (75 mg/kg i.p.) 3 and 14 days after surgery. Blood was collected from the vena cava just before sacrifice by exsanguination, and citrated plasma was stored at −80°C for further analysis. Portions of liver tissue were frozen immediately in liquid nitrogen, whereas others were fixed in 10% neutral buffered formalin for subsequent sectioning and mounting on microscope slides.

Clinical Analyses and Histology. Plasma levels of alanine aminotransferase (ALT), aspartate aminotransferase (AST), alkaline phosphatase (ALP), and bilirubin were determined using standard kits (Thermotrace, Melbourne, Australia). Formalin-fixed, paraffin-embedded sections were cut at 5 μm and mounted on glass slides. Sections were deparaffinized and stained with H&E. Pathologic changes were assessed in a blinded manner. Neutrophil accumulation in the livers was assessed by staining tissue sections for chloracetate esterase, a specific marker for neutrophils, using the naphthol AS-D chloracetate esterase kit (Sigma-Aldrich, St. Louis MO) (Gujral et al., 2004a; Guo et al., 2004). Extracellular matrix accumulation in liver sections was determined by staining with Sirius red-fast green (Lopez-De Leon and Rojkind, 1985).

Sirius red staining was quantified by image analysis. Specifically, a Molecular Devices (Sunnyvale, CA) Image-1/AT image acquisition and analysis system incorporating an Axioskop 50 microscope (Carl Zeiss Inc., Thornwood, NY) was used to capture and analyze five nonoverlapping fields per section at 100× final magnification. Image analysis was performed using modifications of techniques described previously (Arteel et al., 1997). Detection thresholds were set for the red color based on an intensely labeled point and a default color threshold. The degree of labeling in each section was determined from the area within the color range divided by the total area.

Hydroxyproline Determinations. Hydroxyproline content was quantitated colorimetrically from liver samples using the chloramine T method as described by Ellis et al. (1994) with minor modifications. In brief, liver specimens (20–50 mg) were weighed and hydrolyzed in 500 μl of 6 N HCl at 100°C for 24 h. The hydrolysate was then cooled, neutralized with 500 μl of 6 N NaOH, and centrifuged at 13,000*g* for 12 min. Forty microliters of the supernatant was added to a microtiter plate and was incubated with 25 μl of chloramine T solution [1 part 7% chloramine T and 4 parts citrate/acetate buffer (pH 6.0, 695 mM sodium acetate, 128 mM trisodium citrate·2H_2O, and 29 mM citric acid, with 38.5% isopropanol)] at room temperature for 10 min. One hundred fifty microliters of Ehrlich's solution (1.4 M dimethylaminobenzaldehyde with 20% perchloric acid and 67% isopropanol) was then added and incubated at 65°C for 15 min. After cooling, the absorbance was read at 561 nm. Hydroxyproline concentration was calculated from a standard curve prepared with high-purity hydroxyproline. The results were expressed as micrograms of hydroxyproline per gram of liver.

RNA Isolation and Real-Time RT-Polymerase Chain Reaction. Total RNA was extracted from liver tissue samples by a guanidium thiocyanate-based method (RNA STAT 60 Tel-Test; Ambion, Austin, TX). RNA concentrations were determined spectrophotometrically, and 1 μg of total RNA was reverse transcribed using an avian myeloblastosis virus reverse transcriptase kit (Promega, Madison, WI) and random primers. PCR primers and probes were designed using Primer 3 (Whitehead Institute for Biomedical Research, Cambridge, MA; see Table 1). Primers were designed to cross introns to ensure that only cDNA and not DNA was amplified. The fluorogenic minor groove binder probe was labeled with the reporter dye 5-carboxyfluorescein. TaqMan Universal PCR Master Mix (Applied Biosystems, Foster City, CA) was used to prepare the PCR mix. The 2× mixture was optimized for TaqMan reactions and contained AmpliTaq gold DNA polymerase, AmpErase, dNTPs with UTP, and a passive reference. Primers and probe were added to a final concentration of 300 and 100 nM, respectively. The amplification reactions were carried out in the ABI Prism 7700 sequence detection system (Applied Biosystems) with initial hold steps (50°C for 2 min, followed by 95°C for 10 min) and 50 cycles of a two-step PCR (92°C for 15 s, 60°C for 1 min). The fluorescence intensity of each sample was measured at each temperature change to monitor amplification of the target gene. The comparative C_T method was used to determine -fold differences between samples. The comparative C_T method determines the amount of target, normalized to an endogenous reference (β-actin) and relative to a calibrator ($2^{-\Delta\Delta Ct}$). The purity of PCR products were verified by gel electrophoresis.

Determination of Hepatic Plasminogen Activities. The activity of tPA and uPA was determined in liver samples as described by Bezerra et al. (2001). In brief, total protein was extracted from frozen liver tissue samples with phosphate-buffered saline, pH 7.4, containing 1% Nonidet P-40, 0.5% sodium deoxycholate, and 0.1% SDS. Lysates were then diluted in 2× sample buffer (125 mM Tris HCl, pH 6.8, with 4% SDS, 20% glycerol, and 1 mM dithiothreitol) and separated on 12% SDS-polyacrylamide gels containing 2% nonfat dry milk powder (Bio-Rad, Hercules, CA) and 75 mU/ml plasminogen (Sigma-Aldrich). Plasminogen-free gels run in parallel were used to confirm that the activity detected was plasminogen dependent. Gels were incubated twice for 30 min in 2.5% v/v Triton X-100

TABLE 1
Primers and probes used for real-time RT-PCR detection of expression

	Forward (3′–5′)	Reverse (3′–5′)	Probe (3′–5′)
PAI-1	CACCAACATTTTGGACGCTGA	TCAGTCATGCCCAGCTTCTCC	CCAGGCTGCCCCGCCTCCTC
αSMA	TGCCATCATGCGTCTGGACT	GCCGTGGCCATCTCATTTTC	TGCCGAGCGTGAGATTGTCCGTGA
Collagen Iα1	GTCTTCCTGGCCCCTCTGGT	AGCAGGGCCAGTCTCACCAC	CCCCATGGGGCCCCCTGGAT
TIMP-1	CCCACCCACAGACAGCCTTC	CGGCCCGTGATGAGAAACTC	TGCCCACAAGTCCCAGAACCGCA
TIMP-2	CGCCCCTTGACAAAGAGGAC	CTGCATTGCAAAACGCCTGT	TGCAGCTGCTCCCCGGTGCA
β-actin	GGCTCCCAGCACCATGAA	AGCCACCGATCCACACAGA	AAGATCATTGCTCCTCCTGAGCGCAAGTA

solution and washed three times for 30 min in developing solution (50 mM Tris, 0.1 M glycine, and 0.1 M NaCl, pH 8.0) followed by a 16-h incubation in developing buffer at 37°C. The caseinolytic activity was detected by staining the gel (0.1% amido black, 45% methanol, and 10% acetic acid) for 2 h and then destaining (45% methanol and 10% acetic acid) for 30 min. Densitometric analysis was performed using ImageQuant software (GE Healthcare, Little Chalfont, Buckinghamshire, UK).

Determination of MMP-Mediated Collagenase Activities and Plasma TIMP-1 Levels. To determine the hepatic activity of MMPs, total hepatic protein was extracted using a lysis buffer consisting of 10 mM cacodylic acid, pH 5.0, containing 150 mM NaCl, 1 μM ZnCl, 15 mM $CaCl_2$, 1.5 mM NaN_3, and 0.01% Triton X-100. Lysates were then diluted in 2× sample buffer and separated on 10% SDS-polyacrylamide gels containing 0.1% gelatin. Gels were washed, developed, stained, destained, and bands were quantified as described above for uPA and tPA zymography. Plasma TIMP-1 levels were determined using a commercially available kit (Research Diagnostics, Flanders, NJ), which was performed according to manufacturer's instructions. This assay detects both free and bound TIMP-1.

Immunoblots. Protease (20 μM 4-(2-aminoethyl)benzenesulfonyl fluoride, 10 μM EDTA, 1 μg/ml bestatin, 1 μg/ml E-64, 1 μg/ml leupeptin, and 1 μg/ml phenylmethylsulfonyl fluoride), tyrosine phosphatase (1 mM Na_3VO_4, 1.2 mM Na_2MoO_4, 4.8 mM $C_4H_4O_6Na_2$, and 2 mM imidazole), and serine/threonine phosphatase (4.6 μM cantharidin, 20 μM bromotetramisole oxalate, and 0.1 μg/ml microcystin) inhibitors (Sigma-Aldrich) were added to all of the buffers used. For preparation of total hepatic protein, liver samples were homogenized in radioimmunoprecipitation assay buffer (20 mM MOPS, pH 7.0, with 150 mM NaCl, 1 mM EDTA, 1% Nonidet P-40, 1% sodium deoxycholate, and 0.1% SDS). Lysates were then diluted in 2× sample buffer were separated on 8% SDS-polyacrylamide gels. Proteins were transferred to Hybond-P polyvinylidene diflouride membranes (GE Healthcare) using a semidry electroblotter. The resulting blots were then probed with antibodies against phospho-c-Met (Cell Signaling Technology Inc., Beverly, MA), and bands were visualized using an ECL plus kit (GE Healthcare). To ensure equal loading, all blots were stained with Ponceau S red. Haptene signals were normalized to total c-Met using a commercially available antibody (Sigma-Aldrich). Densitometric analysis was performed using ImageQuant software.

Statistical Analyses. Results are reported as means ± S.E.M. ($n = 4–6$). Analysis of variance with Bonferroni's post hoc test or the Mann-Whitney rank sum test was used for the determination of statistical significance among treatment groups, as appropriate. $p < 0.05$ was selected before the study as the level of significance.

Results

Effect of Bile Duct Ligation on Plasma and Histologic Indices of Liver Damage and Fibrosis. In preliminary studies, no differences in parameters of liver damage were observed between wild-type and PAI-$1^{-/-}$ mice after sham surgery; data with the former strain, thus, are shown to represent both. Bilirubin levels in sham-treated animals were normal, with values of ~0.5 mg/dl. In contrast, bilirubin levels were ~8 and 40 mg/dl after 3 days or 2 weeks of bile duct ligation, respectively, and were not significantly different between wild-type and PAI-$1^{-/-}$ mice (Fig. 1, top panel). After 2 weeks of bile duct ligation, the incidence of ascites in wild-type mice was ~70%; no ascites were present in PAI-$1^{-/-}$ mice at this time point.

Plasma levels of indices of liver damage (AST, ALT, and ALP) were within normal ranges in sham-treated mice (Fig. 1, middle and bottom panels). As expected, bile duct ligation significantly increased the levels of these enzymes compared

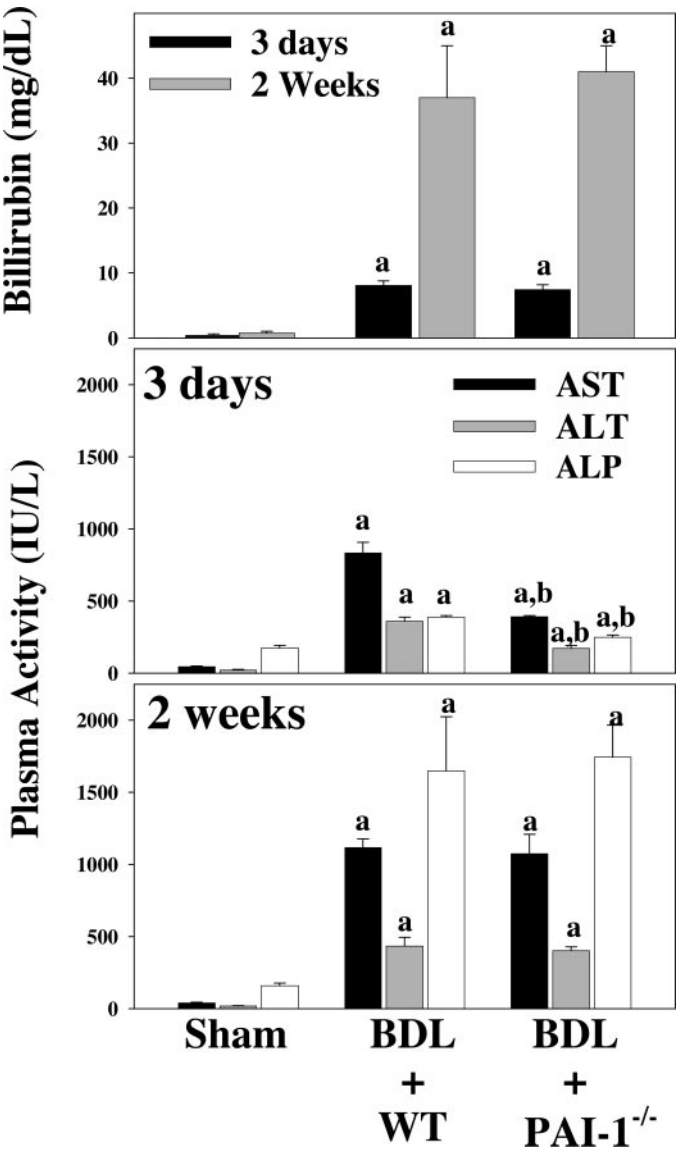

Fig. 1. Effect of bile duct ligation on plasma parameters. Bile duct ligation (BDL) or sham surgery (Sham) was performed in wild-type (WT) and PAI-1 knockout (PAI-$1^{-/-}$) mice as described under *Materials and Methods*. Total bilirubin (top panel) was determined in plasma samples after 3 days (black bars) and 2 weeks (gray bars) of bile duct ligation. AST (black bars), ALT (gray bars), and ALP (white bars) were determined in plasma samples collected after 3 days and 2 weeks of bile duct ligation (middle and bottom panels). Data represent means ± S.E.M. ($n = 4–6$). a, $p < 0.05$ compared with sham surgery; b, $p < 0.05$ compared with wild-type animals subjected to bile duct ligation.

with sham-treated animals. The increase in plasma AST, ALT, and ALP caused by 3 days of bile duct ligation was significantly blunted in PAI-$1^{-/-}$ mice by 40 to 50% (Fig. 1, middle panel). After 2 weeks of bile duct ligation, the levels of these enzymes in plasma of wild-type mice were even greater than at 3 days (Fig. 1, bottom panel). The increase in these parameters after 2 weeks of bile duct ligation was not significantly attenuated in PAI-$1^{-/-}$ mice, with values similar to those in wild-type mice (Fig. 1, bottom panel).

Figure 2 shows representative photomicrographs depicting liver pathology (H&E stain, left column), neutrophil accumulation (chloroacetate esterase stain, center column), and ECM accumulation (Sirius red stain, right column) 3 days and 2 weeks after bile duct ligation (or sham) surgery. No

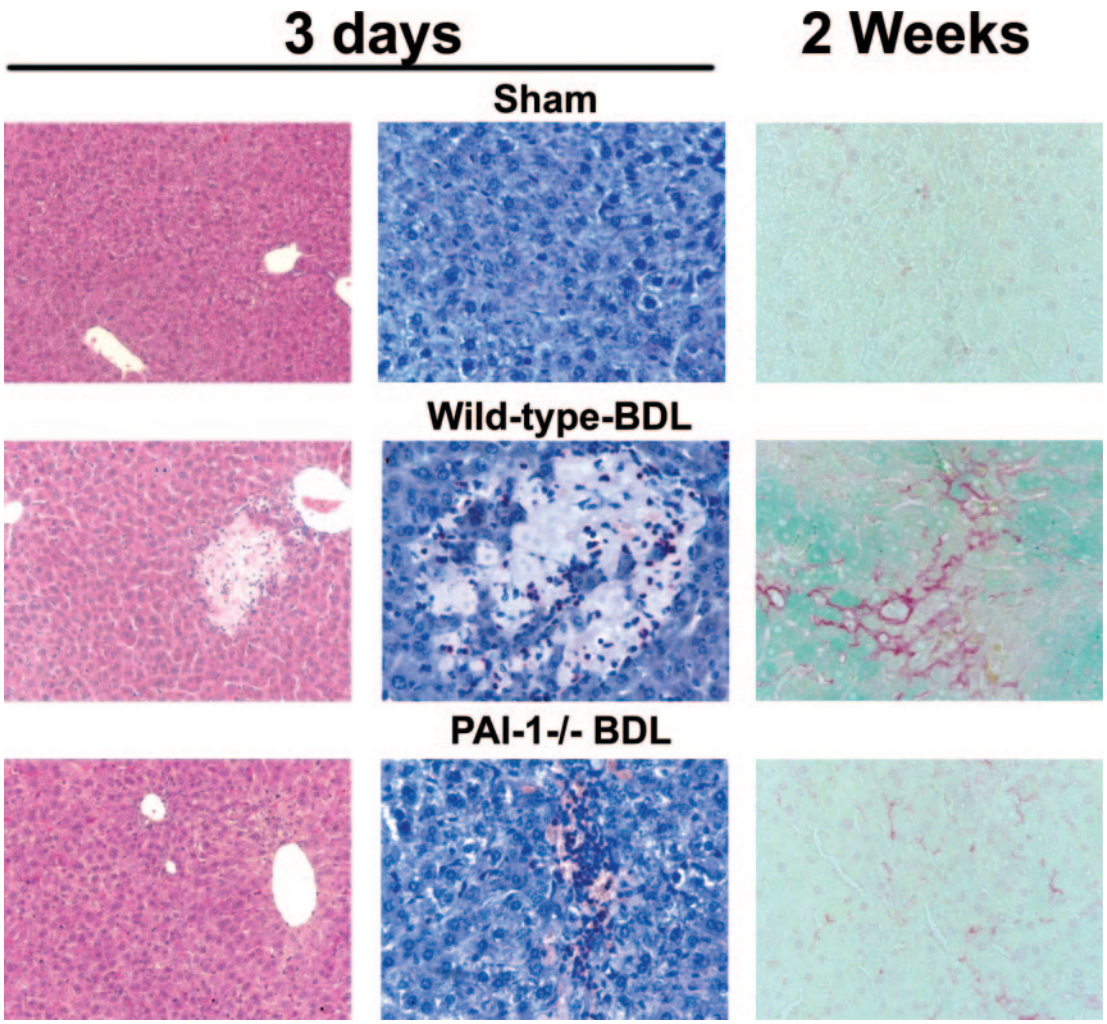

Fig. 2. Photomicrographs of livers following bile duct ligation. Representative photomicrographs of livers from mice that underwent BDL or sham surgery are shown. H&E (100×; left column) and chloroacetate esterase staining (400×; middle column) depict necroinflammatory changes 3 days after the initiation of bile duct ligation. Sirius red (200×; right column) depicts fibrotic changes 2 weeks after the initiation of bile duct ligation.

pathological changes were observed in liver tissue after sham surgery (Fig. 2, top panels). Three days of bile duct ligation caused a robust increase in the incidence of necroinflammatory foci in livers of wild-type mice (Fig. 2, left column, middle panel); these pathologic changes were attenuated in PAI-$1^{-/-}$ mice (Fig. 2, left column, bottom panel). The necroinflammatory foci in livers of wild-type mice after 3 days of bile duct ligation contained numerous neutrophils, as determined by chloroacetate esterase staining (Fig. 2, center column, middle panel). In addition to smaller and fewer necroinflammatory foci, there were also fewer neutrophils within these foci in livers from PAI-$1^{-/-}$ mice (Fig. 2, center column, bottom panel) 3 days after bile duct ligation compared with wild-type animals.

After 2 weeks of bile duct ligation, the accumulation of ECM was easily discernible in livers from wild-type mice stained with Sirius red (Fig. 2, right column, middle panel), whereas still greater than sham-treated animals, the accumulation of extracellular matrix in livers from PAI-$1^{-/-}$ mice (Fig. 2, right column, bottom panel) was significantly suppressed compared with wild-type mice. When quantitated by image analysis (Fig. 3, top panel), Sirius red staining in livers of wild-type mice was ~15% of the total tissue area and was 7-fold higher in comparison with sham-treated mice; the effect of bile duct ligation on this parameter was significantly suppressed by ~60% in livers from PAI-$1^{-/-}$ mice (Fig. 3, top panel). Three days after surgery, hydroxyproline content was similar in all groups, with values of ~100 μg/g tissue. However, 2 weeks of bile duct ligation caused a significant (>2-fold) increase of hydroxyproline in wild-type mice, which was completely attenuated in PAI-$1^{-/-}$ mice (Fig. 3, bottom panel).

Effect of Bile Duct Ligation on the Expression of PAI-1, αSMA, and Collagen Iα1. The induction of PAI-1 is known to increase during hepatic inflammation and fibrosis (e.g., Zhang et al., 1999). Furthermore, increases in the expression of αSMA and collagen Iα1 are indicative of stellate cell activation and ECM synthesis, respectively, in mice after bile duct ligation (e.g., Canbay et al., 2003). Therefore, the effect of bile duct ligation on hepatic expression of these genes was determined in samples from wild-type and PAI-$1^{-/-}$ mice via real-time RT-PCR (Fig. 4). Bile duct ligation led to a significant induction in the expression of all of these parameters in wild-type mice; specifically, 3 days of bile duct ligation led to a 9-, 3-, and 4-fold increase in the expression of PAI-1, αSMA, and collagen Iα1, respectively. As expected,

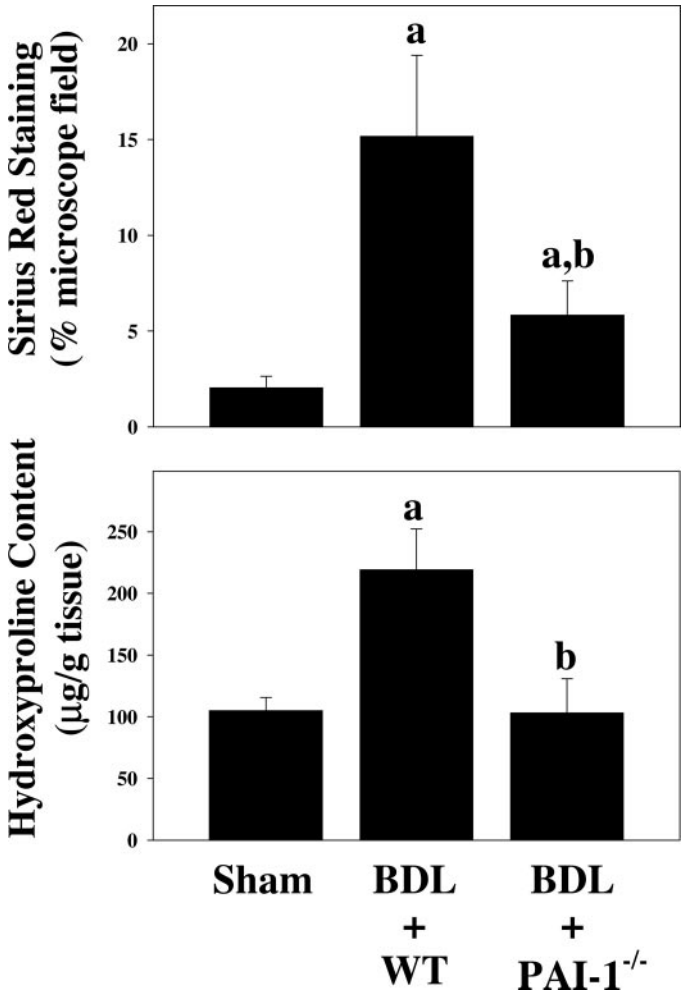

Fig. 3. Quantitation of fibrotic changes after bile duct ligation. BDL or sham surgery (Sham) was performed in wild-type and PAI-1 knockout mice for 2 weeks as described under *Materials and Methods*. The top panel depicts results of image analysis of Sirius red staining as described under *Materials and Methods*. The bottom panel depicts results of colorimetric quantitation of hydroxyproline content in liver tissue as described under *Materials and Methods*. Data represent means ± S.E.M. ($n = 4–6$). a, $p < 0.05$ compared with sham surgery; b, $p < 0.05$ compared with wild-type animals subjected to bile duct ligation.

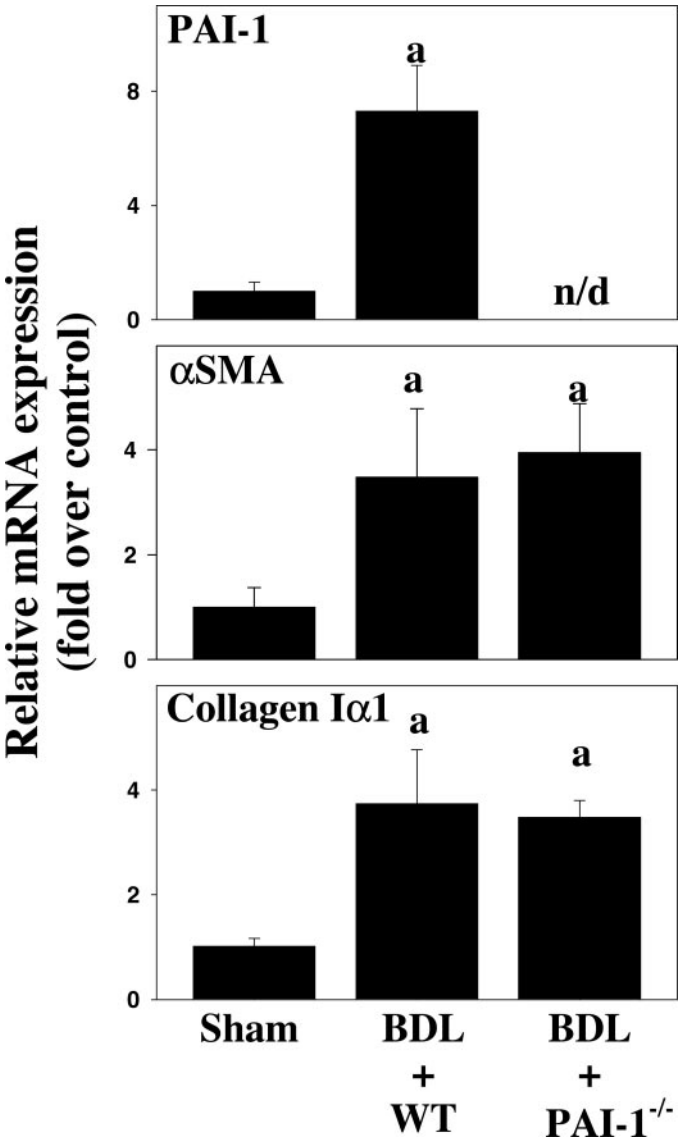

Fig. 4. Effect of bile duct ligation on the expression of PAI-1, αSMA, and collagen Iα1 in mouse liver. BDL or sham surgery (Sham) was performed in wild-type and PAI-1 knockout mice for 3 days as described under *Materials and Methods*. Real-time RT-PCR was performed as described under *Materials and Methods*, and results were normalized to β-actin. Data are means ± S.E.M. ($n = 4–6$) and are reported as -fold over control values. a, $p < 0.05$ compared with sham surgery; b, $p < 0.05$ compared with wild-type animals subjected to bile duct ligation. n/d, not detectable.

the expression of PAI-1 was undetectable in PAI-$1^{-/-}$ mice (Fig. 4, top panel); however, the effect of bile duct ligation on the expression of αSMA (Fig. 4, middle panel) and collagen Iα1 (Fig. 4, bottom panel) was not significantly altered in PAI-$1^{-/-}$ mice. Similar patterns of induction were observed after 2 weeks of bile duct ligation but were highly variable at this time point; for example, induction of αSMA expression after bile duct ligation ranged 6- to 30-fold in comparison with sham mice (data not shown).

Plasminogen Activator and MMP Activity Is Enhanced in PAI-$1^{-/-}$ Mice after Bile Duct Ligation. PAI-1 is a major inhibitor of uPA and tPA, which in turn activates MMPs via plasmin (see Fig. 8 for scheme). Therefore, the activities of uPA and tPA (Fig. 5) and MMP-2 and -9 (Fig. 6) were determined. After 3 days of bile duct ligation, the activity of uPA and tPA (as determined by zymography) was not significantly different between the groups (data not shown). However, after 2 weeks of bile duct ligation, the activity of both enzymes was significantly enhanced in livers of wild-type mice (Fig. 4, top panel); densitometric analysis indicated that tPA and uPA were increased ~50 and 300%, respectively, by bile duct ligation (Fig. 5, middle and bottom panels). The effect of bile duct ligation on the activity of these enzymes was significantly enhanced in PAI-$1^{-/-}$ mice compared with wild-type animals, with values >4-fold over livers from sham-treated mice for both enzymes.

Figure 6 shows representative zymograms for MMP-2 and -9 (top panel), as well as quantification of MMP-2 and -9 activity via densitometric analysis (bottom two panels). Analogous to findings with tPA and uPA, 3 days of bile duct ligation caused no detectable changes in hepatic MMP-2 and -9 activity in either wild-type or PAI-$1^{-/-}$ mice (data not shown). In contrast, a ~2-fold induction in these proteases was observed in livers of wild-type mice after 2 weeks of bile duct ligation. The activities of both isoforms (especially

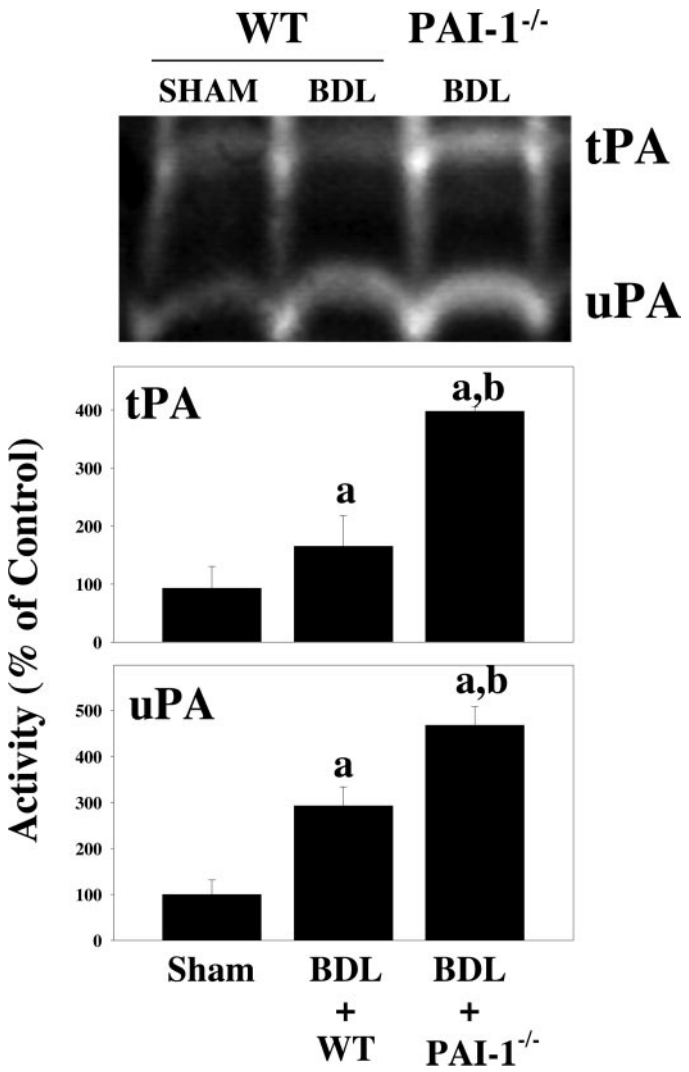

Fig. 5. Effect of bile duct ligation on hepatic tPA and uPA activity in mouse liver. BDL or sham surgery (Sham) was performed in wild-type and PAI-1 knockout mice for 2 weeks as described under *Materials and Methods*. Representative zymographs demonstrating plasmin mediated casein lysis by tPA and uPA are shown in the top panel. The bottom two panels show results of densitometric analysis of activity. Data are means ± S.E.M. (n = 4–6) and are expressed as percentage of control values. a, $p < 0.05$ compared with sham surgery; b, $p < 0.05$ compared with wild-type animals subjected to bile duct ligation.

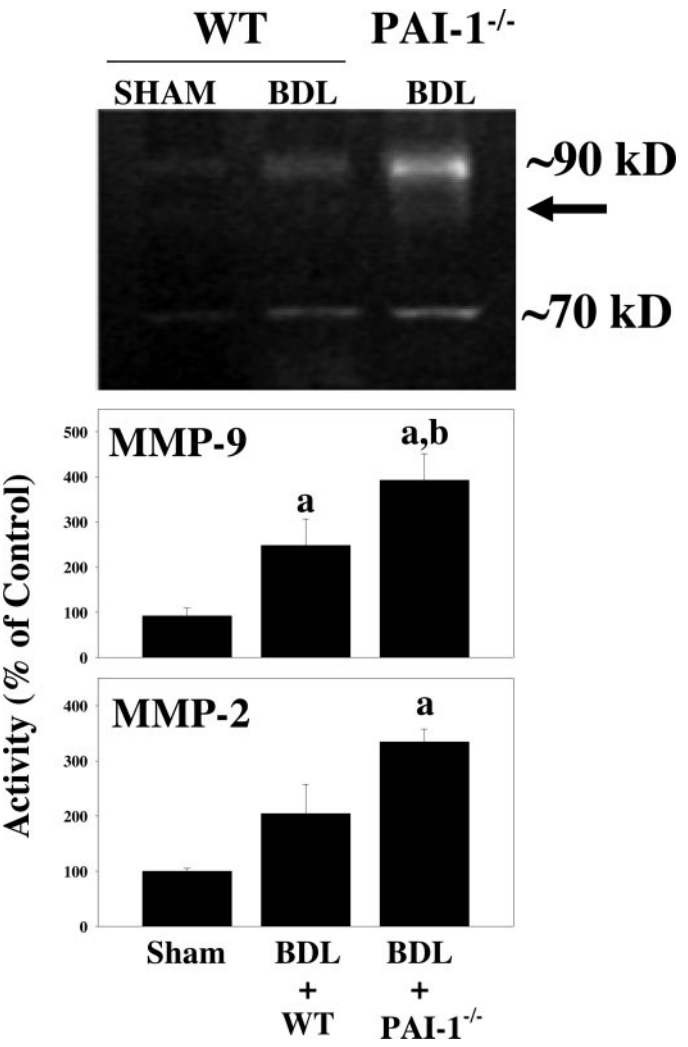

Fig. 6. Effect of bile duct ligation on hepatic MMP-2 and -9 activity in mouse liver. BDL or sham surgery (Sham) was performed in wild-type and PAI-1 knockout mice for 2 weeks as described under *Materials and Methods*. Representative zymographs demonstrating gelatin lysis by MMP-2 and -9 are shown in the top panel. The bottom two panels show results of densitometric analysis of activity. Data are means ± S.E.M. (n = 4–6) and are expressed as percentage of control values. a, $p < 0.05$ compared with sham surgery; b, $p < 0.05$ compared with wild-type animals subjected to bile duct ligation.

MMP-9) were induced to a significantly greater extent by bile duct ligation in livers from PAI-$1^{-/-}$ mice. Furthermore, a lower mol. wt. band corresponding to "active" MMP-9 was observed in samples from PAI-$1^{-/-}$ mice after 2 weeks of bile duct ligation (Fig. 6, top panel, arrow) but was too faint for quantification by densitometry.

Bile Duct Ligation Induced TIMP-1 to a Similar Extent in Wild-Type and PAI-$1^{-/-}$ Mice. The activity of MMPs in vivo is controlled not only by activation of the latent enzymes but also by inhibition of the active enzyme by TIMPs. Indeed, antibodies against TIMP-1 were recently shown to enhance the rate of recovery from CCl_4-induced fibrosis in rats (Parsons et al., 2004). Therefore, the effects of bile duct ligation on hepatic expression (real-time RT-PCR) and plasma protein levels (enzyme-linked immunosorbent assay) of TIMP-1 were determined (Fig. 7). Two weeks of bile duct ligation significantly increased TIMP-1 message and protein levels by ~40- and ~5-fold, respectively, in wild-type mice. The induction of TIMP-1 caused by bile duct ligation was not altered in PAI-$1^{-/-}$ mice in comparison with wild-type animals (Fig. 7). The expression of TIMP-2 in liver was not significantly altered by 2 weeks of bile duct ligation with a -fold expression (relative to sham-treated mice) of 1.1 ± 0.1 and 0.9 ± 0.2 in wild-type and PAI-$1^{-/-}$ mice, respectively.

Phosphorylation of c-Met Is Enhanced in PAI-$1^{-/-}$ Mice after Bile Duct Ligation. In addition to activating plasminogen, uPA has also been shown to activate prohepatocyte growth factor (HGF) to mature HGF (Naldini et al., 1995; Taniyama et al., 2000), which can then bind and activate its receptor c-Met (Bottaro et al., 1991). Therefore, the effect of bile duct ligation and knocking out PAI-1 on total c-Met and activation (phosphorylation) was determined in liver tissue by Western blot (Fig. 8). In wild-type mice, bile duct ligation did not alter the amount of detectable phospho c-Met but significantly decreased the amount of total, leading

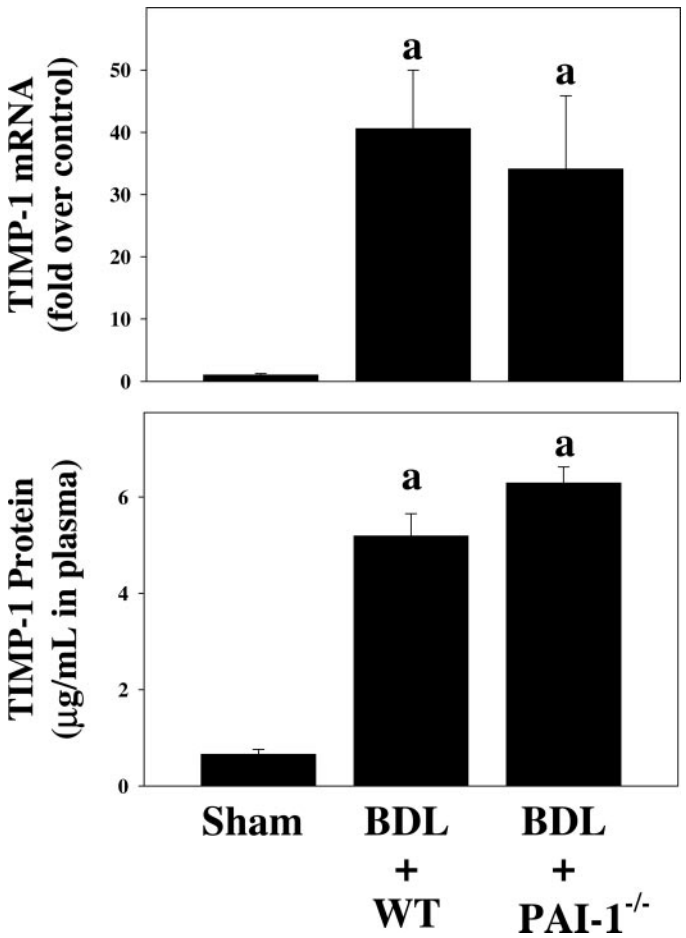

Fig. 7. Effect of bile duct ligation on plasma TIMP-1 expression and protein levels. BDL or sham surgery (Sham) was performed in wild-type and PAI-1 knockout mice for 2 weeks as described under *Materials and Methods*. Real-time RT-PCR (top panel) was performed as described under *Materials and Methods*, and results were normalized to β-actin. Enzyme-linked immunosorbent assay for mouse TIMP-1 (bottom panel) was performed in plasma was performed using commercially available kits. Data are means ± S.E.M. (n = 4–6). a, $p < 0.05$ compared with sham surgery.

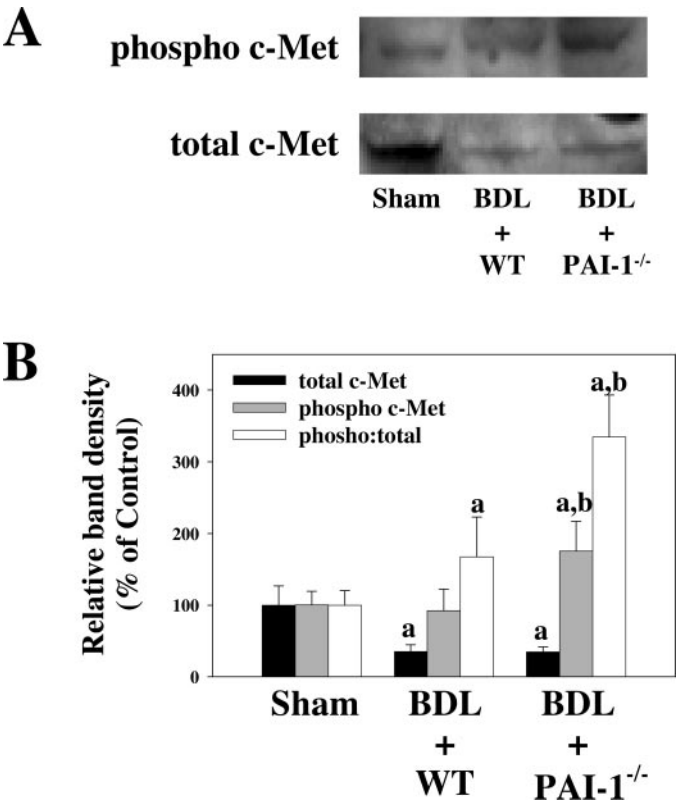

Fig. 8. Effect of bile duct ligation on phosphorylation of c-Met. BDL or sham surgery (Sham) was performed in wild-type and PAI-1 knockout mice for 2 weeks as described under *Materials and Methods*. Western blot performed as described under *Materials and Methods*. Representative Western blots for phospho-c-Met and total c-Met are shown in A. B, results of densitometric analysis of band intensities and the ratio of phospho-c-Met to total. Data are means ± S.E.M. (n = 4–6). a, $p < 0.05$ compared with sham surgery; b, $p < 0.05$ compared with wild-type animals subjected to bile duct ligation.

to a net increase in the ratio of total:phospho. Although total c-Met was also decreased in livers from PAI-$1^{-/-}$ mice, there was also a concomitant increase in phospho c-Met under these conditions. The ratio of phospho:total was significantly greater in this strain than in any other treatment group.

Discussion

PAI-$1^{-/-}$ Mice Are Protected from Cholestasis-Induced Liver Damage and Fibrosis. The major findings of this study relate PAI-1 expression to liver injury and fibrogenesis in a mouse model of cholestatic liver injury. Specifically, it was shown that PAI-1 is induced by bile duct ligation in mice as early as 3 days after surgery (Fig. 3). Furthermore, PAI-$1^{-/-}$ mice were protected against early increases in liver damage, as determined by plasma enzyme release (Fig. 1) and histologic assessment (Fig. 2, left panels). It should be noted that the hepatoprotective effect of this knockout seems to be transient because plasma enzyme levels were not significantly attenuated in PAI-$1^{-/-}$ mice 2 weeks after bile duct ligation (see below). In contrast, PAI-$1^{-/-}$ mice were dramatically protected against ECM accumulation after 2 weeks of bile duct ligation, as determined by histological (Figs. 2 and 3, top panel) assessment as well as by hydroxyproline content (Fig. 3, bottom panel).

As described above, previous studies have identified a causal role of PAI-1 in fibrosis of kidneys, lungs, and the vascular. In liver, a correlation between PAI-1 levels and protection against fibrosis has been observed. For example, Bueno et al. (2000) observed a correlation among PAI-1 levels, MMP activity, and protection against cholestasis-induced liver fibrosis by interferon α-2a. However, a specific causal role of PAI-1 in hepatic fibrogenesis in vivo had not been directly determined prior to the current work. Based on studies with isolated and cultured stellate cells, Leyland et al. (1996) proposed that PAI-1 may be both antifibrotic and profibrotic in liver, the former being mediated by the inhibition of interstitial collagenases during early stages of fibrosis. The data shown here clearly support the hypothesis that PAI-1 is predominantly profibrotic in liver in vivo, at least in response to bile duct ligation in the mouse.

As mentioned above, PAI-1 has been shown to be induced in other animal models of hepatic fibrosis (Zhang et al., 1999). However, in addition to differences in the pattern of fibrosis between bile duct ligation and toxin-induced (e.g., CCl_4) fibrosis, hepatocyte death and inflammation are generally more robust in the latter models compared with bile duct ligation (Galli et al., 2002; Lotersztajn et al., 2005).

Thus, whether or not PAI-1 is broadly involved in hepatic fibrogenesis cannot be determined from the results of the current work. Although a direct role of PAI-1 in toxin-induced hepatic fibrosis has not been determined, previous studies investigating the plasminogen system indirectly support such a possible function. For example, genetic deletion of plasminogen has been shown to exacerbate hepatic fibrogenesis in response to CCl_4 (Ng et al., 2001). Furthermore, increasing the conversion of plasminogen to plasmin by adenoviral overexpression of uPA in rat liver has been shown to accelerate the recovery from CCl_4-induced liver fibrosis (Salgado et al., 2000).

PAI-1$^{-/-}$ Mice Are Protected Independent of ECM Production. There are multiple levels at which hepatic fibrosis is regulated (Bataller and Brenner, 2005). A major source of regulation is the transformation of stellate cells to myofibroblasts and production of ECM by these cells. To test the hypothesis that the protective effect of knocking PAI-1 was mediated at this level, the expression of known indices of this process (αSMA and collagen Iα1) was determined. As expected, bile duct ligation caused a robust increase in the expression of these parameters, but this effect was not significantly attenuated in PAI-1$^{-/-}$ mice (Fig. 3). Therefore, it seems unlikely that knocking out PAI-1 confers protection against hepatic fibrosis caused by bile duct ligation via regulation of the above-described processes.

How Are PAI-1$^{-/-}$ Mice Protected from Cholestasis-Induced Liver Damage and Fibrosis? As described above, PAI-1$^{-/-}$ mice were protected against early (3 days) liver damage caused by bile duct ligation, as determined by serum enzyme release (Fig. 1) and histologic evaluation (Fig. 2). Work by others has shown that liver damage at this time point after bile duct ligation is mediated predominantly by hepatic inflammation in general (Gujral et al., 2004b) and neutrophil accumulation in particular (Gujral et al., 2003, 2004a). Here, it was observed that after 3 days of bile duct ligation, hepatic infiltration of neutrophils was attenuated in PAI-1$^{-/-}$ mice (see Fig. 2). A similar correlation between protection against tissue damage and attenuation of neutrophil recruitment has been observed with PAI-1$^{-/-}$ mice in acute lung damage caused by lipopolysaccharide (Arndt et al., 2005). PAI-1 has also been shown to be permissive to neutrophil transendothelial migration in vitro, most likely via prevention of the degradation of IL-8 (Marshall et al., 2003). Therefore, it is likely that the protective effect against bile duct ligation-induced liver damage at this time point is mediated via a blunting of neutrophil accumulation in the liver. The lack of protection in PAI-1$^{-/-}$ mice later in the model (i.e., after 2 weeks of bile duct ligation) may be due to the relatively higher levels of bile acids at this time point (see Fig. 1) causing significant direct toxicity to the organ.

In addition to regulating synthesis of ECM, hepatic fibrogenesis is also determined by the balance between enzymes that degrade ECM (e.g., MMPs) and their inhibitors (e.g., TIMPs) (Arthur, 2000). To determine whether or not PAI-1$^{-/-}$ mice are protected against hepatic fibrosis at this level, the effects of bile duct ligation on MMP-2 and -9 activity (Fig. 6), as well as on TIMP-1 levels (Fig. 7), were compared between wild-type and PAI-1$^{-/-}$ mice. Indeed, although collagenase (MMP-2 and -9) activity was only moderately increased by bile duct ligation in wild-type mice, bile duct ligation led to significant increase of MMP-2 and -9 activities in PAI-1$^{-/-}$ mice (Fig. 6). However, the robust induction of TIMP-1 mRNA and protein by bile duct ligation was similar in wild-type and PAI-1$^{-/-}$ mice (Fig. 7). Therefore, the increase in MMP activity observed in PAI-1$^{-/-}$ mice cannot be explained by prevention of the induction of TIMPs.

In addition to the inhibition of activity by TIMPs, MMPs are also regulated by their conversion from the latent state to active form by other proteases (e.g., plasmin; see Fig. 9). Because PAI-1 is a known inhibitor of the major activators of plasmin in the liver (i.e., uPA and tPA), the effect of bile duct ligation on the activation of these proteases was also determined in wild-type and PAI-1$^{-/-}$ mice (Fig. 5). Although bile duct ligation increased the activity of these proteases, the induction caused by bile duct ligation was much greater in PAI-1$^{-/-}$ mice compared with wild-type mice. Taken together, these data support the hypothesis that PAI-1$^{-/-}$ mice are protected against cholestasis-induced liver injury via an enhanced activation of proteases that degrade ECM (see Fig. 9).

In addition to modulating ECM degradation, PAI-1 may indirectly mediate hepatic fibrogenesis caused by bile duct ligation via prevention of the activation of HGF by uPA (Naldini et al., 1995). In support of this hypothesis, increasing hepatic HGF levels via adenoviral expression also have been shown to enhance the rate of recovery from experimental fibrosis and cirrhosis in rats (Ueki et al., 1999; Lin et al., 2005). In the present study, total c-Met was decreased by bile duct ligation, and the phosphorylation of c-Met was significantly enhanced in PAI-1$^{-/-}$ mice (Fig. 8). Taken together, these results add further support to the hypothesis that HGF/c-Met are involved in protection from fibrosis in the liver.

In summary, a robust protection against hepatic fibrosis was observed in mice deficient in PAI-1. Recent studies have identified a beneficial role of inhibiting TIMPs in CCl_4-induced fibrosis in rats (Parsons et al., 2004). The data shown here suggest that agents that target the induction or activity of PAI-1 may also be beneficial and/or complementary to drugs that target TIMP activation. Whether or not PAI-1 is specific to cholestasis-induced fibrosis or is broadly involved in hepatic fibrogenesis is the focus of future studies. Further-

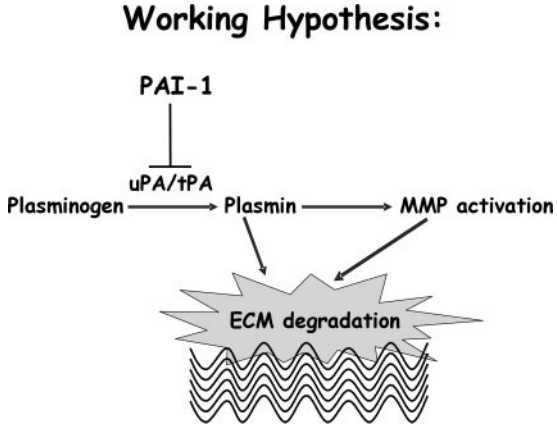

Fig. 9. Proposed mechanism by which PAI-1 contributes to hepatic fibrosis. PAI-1 is induced during fibrogenesis and is a potent inhibitor of the plasminogen activators (tPA and uPA), which convert plasminogen to plasmin. Plasmin can indirectly degrade ECM via activation of MMPs. Plasmin can also potentially directly degrade ECM components (e.g., fibrin, fibronectin, laminin, proteoglycan, and type IV collagen).

more, most studies in humans thus far have focused on the role of the plasminogen system on the development of the hyperfibrinolytic state with advanced liver cirrhosis (e.g., Toschi et al., 1993). Whether or not PAI-1 contributes to the initiation and progression of fibrosis in humans should be investigated.

References

Arndt PG, Young SK, and Worthen GS (2005) Regulation of lipopolysaccharide-induced lung inflammation by plasminogen activator inhibitor-1 through a JNK-mediated pathway. *J Immunol* **175:**4049–4059.

Arteel GE, Iimuro Y, Yin M, Raleigh JA, and Thurman RG (1997) Chronic enteral ethanol treatment causes hypoxia in rat liver tissue *in vivo*. *Hepatology* **25:**920–926.

Arthur MJ (2000) Fibrogenesis: II. Metalloproteinases and their inhibitors in liver fibrosis. *Am J Physiol* **279:**G245–G249.

Bataller R and Brenner DA (2005) Liver fibrosis. *J Clin Investig* **115:**209–218.

Bezerra JA, Currier AR, Melin-Aldana H, Sabla G, Bugge TH, Kombrinck KW, and Degen JL (2001) Plasminogen activators direct reorganization of the liver lobule after acute injury. *Am J Pathol* **158:**921–929.

Bottaro DP, Rubin JS, Faletto DL, Chan AM, Kmiecik TE, Vande Woude GF, and Aaronson SA (1991) Identification of the hepatocyte growth factor receptor as the c-met proto-oncogene product. *Science (Wash DC)* **251:**802–804.

Bueno MR, Daneri A, and Armendariz-Borunda J (2000) Cholestasis-induced fibrosis is reduced by interferon alpha-2a and is associated with elevated liver metalloprotease activity. *J Hepatol* **33:**915–925.

Canbay A, Guicciardi ME, Higuchi H, Feldstein A, Bronk SF, Rydzewski R, Taniai M, and Gores GJ (2003) Cathepsin B inactivation attenuates hepatic injury and fibrosis during cholestasis. *J Clin Investig* **112:**152–159.

Ellis AJ, Curry VA, Powell EK, and Cawston TE (1994) The prevention of collagen breakdown in bovine nasal cartilage by TIMP, TIMP-2 and a low molecular weight synthetic inhibitor. *Biochem Biophys Res Commun* **201:**94–101.

Galli A, Crabb DW, Ceni E, Salzano R, Mello T, Svegliati-Baroni G, Ridolfi F, Trozzi L, Surrenti C, and Casini A (2002) Antidiabetic thiazolidinediones inhibit collagen synthesis and hepatic stellate cell activation in vivo and in vitro. *Gastroenterology* **122:**1924–1940.

Gujral JS, Farhood A, Bajt ML, and Jaeschke H (2003) Neutrophils aggravate acute liver injury during obstructive cholestasis in bile duct-ligated mice. *Hepatology* **38:**355–363.

Gujral JS, Liu J, Farhood A, Hinson JA, and Jaeschke H (2004a) Functional importance of ICAM-1 in the mechanism of neutrophil-induced liver injury in bile duct-ligated mice. *Am J Physiol* **286:**G499–G507.

Gujral JS, Liu J, Farhood A, and Jaeschke H (2004b) Reduced oncotic necrosis in Fas receptor-deficient C57BL/6J-lpr mice after bile duct ligation. *Hepatology* **40:**998–1007.

Guo L, Richardson KS, Tucker LM, Doll MA, Hein DW, and Arteel GE (2004) Role of the renin-angiotensin system in hepatic ischemia reperfusion injury in rats. *Hepatology* **40:**583–589.

Hattori N, Degen JL, Sisson TH, Liu H, Moore BB, Pandrangi RG, Simon RH, and Drew AF (2000) Bleomycin-induced pulmonary fibrosis in fibrinogen-null mice. *J Clin Investig* **106:**1341–1350.

Huang Y, Haraguchi M, Lawrence DA, Border WA, Yu L, and Noble NA (2003) A mutant, noninhibitory plasminogen activator inhibitor type 1 decreases matrix accumulation in experimental glomerulonephritis. *J Clin Investig* **112:**379–388.

Kaikita K, Fogo AB, Ma L, Schoenhard JA, Brown NJ, and Vaughan DE (2001) Plasminogen activator inhibitor-1 deficiency prevents hypertension and vascular fibrosis in response to long-term nitric oxide synthase inhibition. *Circulation* **104:**839–844.

Kim WR, Brown RS Jr, Terrault NA, and El Serag H (2002) Burden of liver disease in the United States: summary of a workshop. *Hepatology* **36:**227–242.

Kruithof EK (1988) Plasminogen activator inhibitors: a review. *Enzyme* **40:**113–121.

Lagoa CE, Vodovotz Y, Stolz DB, Lhuillier F, McCloskey C, Gallo D, Yang R, Ustinova E, Fink MP, Billiar TR, et al. (2005) The role of hepatic type 1 plasminogen activator inhibitor (PAI-1) during murine hemorrhagic shock. *Hepatology* **42:**390–399.

Leyland H, Gentry J, Arthur MJ, and Benyon RC (1996) The plasminogen-activating system in hepatic stellate cells. *Hepatology* **24:**1172–1178.

Lin Y, Xie WF, Chen YX, Zhang X, Zeng X, Qiang H, Chen WZ, Yang XJ, Han ZG, and Zhang ZB (2005) Treatment of experimental hepatic fibrosis by combinational delivery of urokinase-type plasminogen activator and hepatocyte growth factor genes. *Liver Int* **25:**796–807.

Liotta LA, Goldfarb RH, Brundage R, Siegal GP, Terranova V, and Garbisa S (1981) Effect of plasminogen activator (urokinase), plasmin and thrombin on glycoprotein and collagenous components of basement membrane. *Cancer Res* **41:**4629–4636.

Lopez-De Leon A and Rojkind M (1985) A simple micromethod for collagen and total protein determination in formalin-fixed paraffin-embedded sections. *J Histochem Cytochem* **33:**737–743.

Lotersztajn S, Julien B, Teixeira-Clerc F, Grenard P, and Mallat A (2005) Hepatic fibrosis: molecular mechanisms and drug targets. *Annu Rev Pharmacol Toxicol* **45:**605–628.

Luyendyk JP, Maddox JF, Green CD, Ganey PE, and Roth RA (2004) Role of hepatic fibrin in idiosyncrasy-like liver injury from lipopolysaccharide-ranitidine coexposure in rats. *Hepatology* **40:**1342–1351.

Mackay AR, Corbitt RH, Hartzler JL, and Thorgeirsson UP (1990) Basement membrane type IV collagen degradation: evidence for the involvement of a proteolytic cascade independent of metalloproteinases. *Cancer Res* **50:**5997–6001.

Marshall LJ, Ramdin LS, Brooks T, DPhil PC, and Shute JK (2003) Plasminogen activator inhibitor-1 supports IL-8-mediated neutrophil transendothelial migration by inhibition of the constitutive shedding of endothelial IL-8/heparan sulfate/syndecan-1 complexes. *J Immunol* **171:**2057–2065.

Mochan E and Keler T (1984) Plasmin degradation of cartilage proteoglycan. *Biochim Biophys Acta* **800:**312–315.

Naldini L, Vigna E, Bardelli A, Follenzi A, Galimi F, and Comoglio PM (1995) Biological activation of pro-HGF (hepatocyte growth factor) by urokinase is controlled by a stoichiometric reaction. *J Biol Chem* **270:**603–611.

Ng VL, Sabla GE, Melin-Aldana H, Kelley-Loughnane N, Degen JL, and Bezerra JA (2001) Plasminogen deficiency results in poor clearance of non-fibrin matrix and persistent activation of hepatic stellate cells after an acute injury. *J Hepatol* **35:**781–789.

Parsons CJ, Bradford BU, Pan CQ, Cheung E, Schauer M, Knorr A, Krebs B, Kraft S, Zahn S, Brocks B, et al. (2004) Antifibrotic effects of a tissue inhibitor of metalloproteinase-1 antibody on established liver fibrosis in rats. *Hepatology* **40:**1106–1115.

Poynard T, McHutchison J, Manns M, Trepo C, Lindsay K, Goodman Z, Ling MH, and Albrecht J (2002) Impact of pegylated interferon α-2b and ribavirin on liver fibrosis in patients with chronic hepatitis C. *Gastroenterology* **122:**1303–1313.

Quax PH, van den Hoogen CM, Verheijen JH, Padro T, Zeheb R, Gelehrter TD, van Berkel TJ, Kuiper J, and Emeis JJ (1990) Endotoxin induction of plasminogen activator and plasminogen activator inhibitor type 1 mRNA in rat tissues in vivo. *J Biol Chem* **265:**15560–15563.

Ramos-DeSimone N, Hahn-Dantona E, Sipley J, Nagase H, French DL, and Quigley JP (1999) Activation of matrix metalloproteinase-9 (MMP-9) via a converging plasmin/stromelysin-1 cascade enhances tumor cell invasion. *J Biol Chem* **274:**13066–13076.

Salgado S, Garcia J, Vera J, Siller F, Bueno M, Miranda A, Segura A, Grijalva G, Segura J, Orozco H, et al. (2000) Liver cirrhosis is reverted by urokinase-type plasminogen activator gene therapy. *Mol Ther* **2:**545–551.

Taniyama Y, Morishita R, Nakagami H, Moriguchi A, Sakonjo H, Shokei K, Matsumoto K, Nakamura T, Higaki J, and Ogihara T (2000) Potential contribution of a novel antifibrotic factor, hepatocyte growth factor, to prevention of myocardial fibrosis by angiotensin II blockade in cardiomyopathic hamsters. *Circulation* **102:**246–252.

Toschi V, Rocchini GM, Motta A, Fiorini GF, Cimminiello C, Violi F, Castelli C, Sironi D, and Gibelli A (1993) The hyperfibrinolytic state of liver cirrhosis: possible pathogenetic role of ascites. *Biomed Pharmacother* **47:**345–352.

Ueki T, Kaneda Y, Tsutsui H, Nakanishi K, Sawa Y, Morishita R, Matsumoto K, Nakamura T, Takahashi H, Okamoto E, et al. (1999) Hepatocyte growth factor gene therapy of liver cirrhosis in rats. *Nat Med* **5:**226–230.

Zhang LP, Takahara T, Yata Y, Furui K, Jin B, Kawada N, and Watanabe A (1999) Increased expression of plasminogen activator and plasminogen activator inhibitor during liver fibrogenesis of rats: role of stellate cells. *J Hepatol* **31:**703–711.

Address correspondence to: Dr. Gavin E. Arteel, Department of Pharmacology and Toxicology, University of Louisville Health Sciences Center, Louisville, KY 40292. E-mail: gavin.arteel@louisville.edu